

# Multiple-octave spanning high-energy mid-IR supercontinuum generation in bulk quadratic nonlinear crystals

**Zhou, Binbin; Bache, Morten**

*Published in:*
APL Photonics

*Link to article, DOI:*
10.1063/1.4953177

*Publication date:*
2016

*Document Version*
Publisher's PDF, also known as Version of record

AIP | APL Photonics

# Invited Article: Multiple-octave spanning high-energy mid-IR supercontinuum generation in bulk quadratic nonlinear crystals

Binbin Zhou and Morten Bache

Citation: APL Photonics **1**, 050802 (2016); doi: 10.1063/1.4953177
View online: http://dx.doi.org/10.1063/1.4953177
View Table of Contents: http://scitation.aip.org/content/aip/journal/app/1/5?ver=pdfcov
Published by the AIP Publishing



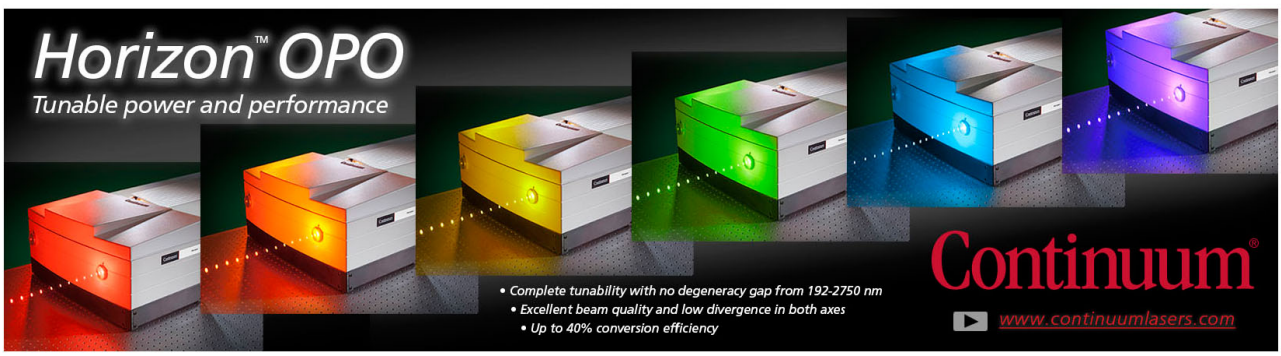

# Invited Article: Multiple-octave spanning high-energy mid-IR supercontinuum generation in bulk quadratic nonlinear crystals

Binbin Zhou and Morten Bache[a]
*DTU Fotonik, Department of Photonics Engineering, Technical University of Denmark, DK-2800 Kgs. Lyngby, Denmark*

(Received 18 March 2016; accepted 21 May 2016; published online 23 June 2016)

Bright and broadband coherent mid-IR radiation is important for exciting and probing molecular vibrations. Using cascaded nonlinearities in conventional quadratic nonlinear crystals like lithium niobate, self-defocusing near-IR solitons have been demonstrated that led to very broadband supercontinuum generation in the visible, near-IR, and short-wavelength mid-IR. Here we conduct an experiment where a mid-IR crystal is pumped in the mid-IR. The crystal is cut for noncritical interaction, so the three-wave mixing of a single mid-IR femtosecond pump source leads to highly phase-mismatched second-harmonic generation. This self-acting cascaded process leads to the formation of a self-defocusing soliton at the mid-IR pump wavelength and after the self-compression point multiple octave-spanning supercontinua are observed. The results were recorded in a commercially available crystal $LiInS_2$ pumped in the 3-4 $\mu$m range with 85 fs 50 $\mu$J pulse energy, with the broadest supercontinuum covering 1.6-7.0 $\mu$m. We measured up 30 $\mu$J energy in the supercontinuum, and the energy promises to scale favorably with an increased pump energy. Other mid-IR crystals can readily be used as well to cover other pump wavelengths and target other supercontinuum wavelength ranges. 
[http://dx.doi.org/10.1063/1.4953177]

## I. INTRODUCTION

High-power supercontinuum sources[1] are laser pulses that have achieved octave-spanning broadened spectra by passing the laser through a bulk nonlinear medium. They are widely used in spectroscopy as broadband "white-light" probes that in a single shot can assess a wide range of frequencies. Recently, a significant effort has been put into investigating supercontinuum generation in the mid-infrared (mid-IR) range, spanning from 3.0 to 20.0 $\mu$m, because it holds a tremendous scientific and technological potential. It contains the fundamental frequencies of vibrational stretching modes of the important C–H, O–H, and N–H bonds that lie in the 2.5-3.5 $\mu$m wavelength range, and the carbon doublet and triplets in the 4-7 $\mu$m range. From 7 to 20 $\mu$m lies the so-called fingerprint region where all organic compounds have a unique spectral absorption pattern due to single-bond bending modes. With a broadband mid-IR supercontinuum the vibrational modes can be probed with femtosecond resolution,[2] but currently these sources do not contain enough energy to use them for broadband pumping.

Unlike most fiber-based supercontinuum sources, which rely on soliton formation,[3] the bulk supercontinuum source relies mainly on broadening induced by self-phase modulation (SPM). At high powers a filament is created by the intense laser pulse. This happens because the beam experiences focusing to a small spot by the nonlinear self-focusing Kerr-lens effect that arises

[a]moba@fotonik.dtu.dk. URL: www.fotonik.dtu.dk/uno.

 

because the Kerr nonlinear refractive index is positive. Multiple filamentation is often undesirable as it can lead to a spatially incoherent beam. However, under controlled circumstances a so-called white-light continuum can be generated, where typically a single filament is created ensuring a good spatial coherence.[4] Both the SPM-induced broadening and the white-light continuum techniques are widely used in the near-IR but little has been done in the mid-IR: Broadband continua were found when pumping with mid-IR pulses through SPM alone (i.e., before filamentation set in),[5,6] which is limited in energy by the onset of small-scale filamentation, or by generating a white-light continuum by an increased peak power.[7–11] This is inevitably limited in energy of a single filament, i.e., to a few $\mu$J. Recent studies also report on mid-IR pulse self-compression and supercontinuum generation in the regime of strong anomalous dispersion,[12] but the role of filamentation is presently not clear. Another approach used a $CO_2$ picosecond laser at $\lambda = 10$ $\mu$m where a supercontinuum formed due to sub-picosecond pulse splitting. Finally, one may start with a femtosecond near-IR source and mix the frequency-converted harmonics in air and use four-wave mixing to achieve broadband mid-IR radiation,[13,14] but with a very low yield.

As an alternative route, supercontinuum generation has been observed in bulk quadratic nonlinear crystals.[15–18] Around phase-matching the pump spectral broadening is accompanied by second-harmonic generation (SHG), which adds to the spectral bandwidth. However, even when tuning away from SHG phase matching ($\Delta k = k_2 - 2k_1 \neq 0$) the spectral broadening can become surprisingly large. This has two likely explanations: 1) the SPM initiated continuum around the pump can mix through sum-frequency generation with the pump. 2) The phase-mismatched SHG process generates a "cascaded" Kerr-like cubic nonlinearity $n_{2,\mathrm{casc}} \propto -d_{\mathrm{eff}}^2/\Delta k$. This contributes to the material Kerr SPM nonlinearity, $n_{2,\mathrm{Kerr}}$, which is self-focusing, to give an overall effective nonlinearity $n_{2,\mathrm{eff}} = n_{2,\mathrm{casc}} + n_{2,\mathrm{Kerr}}$. For $\Delta k < 0$ the cascaded effect is also self-focusing, so the supercontinuum is in bulk often accompanied by filamentation. Conversely, for $\Delta k > 0$ the cascaded nonlinearity becomes self-defocusing, and under the right pumping conditions the effective nonlinearity becomes self-defocusing as well, $n_{2,\mathrm{eff}} < 0$. It is this case we will investigate here. Since the effective nonlinearity is self-defocusing the supercontinuum is filament-free and thus no longer constrained to the filament energy limit of a few $\mu$J.

We recently showed a filament-free supercontinuum in bulk lithium niobate (LN).[19] LN is particularly interesting because it exploits "noncritical" $ee \rightarrow e$ three-wave mixing to achieve cascading through the large diagonal quadratic nonlinear tensor component ($d_{33} \simeq 25$ pm/V), with the additional advantage of zero spatial walk-off to the second-harmonic. The spectral broadening was very large (octave spanning, recently even up to 1.5 octaves was observed[20]) because it was possible to excite solitons when pumping in the near-IR in the normal dispersion regime of LN.

Here we show that multiple-octave spanning mid-IR supercontinua with 10 s of $\mu$J of energy can be generated in a crystal similar to LN but transparent in most of the mid-IR. The crystal, lithium thioindate ($LiInS_2$, LIS), is pumped with ~50 $\mu$J sub-100 fs pulses from 3.0 to 3.9 $\mu$m around its zero-dispersion wavelength (ZDW), resulting in supercontinua spanning well over 2 octaves, which importantly retain most of the pump pulse energy. The spectra are broad enough to cover the range 2.5-6.0 $\mu$m in a single pulse, which is important to probe fundamental vibrations of O–H, C–H, N–H, O–D, metallic C–O, and organic C–O bonds, all in a single pulse.

## II. KERR-LIKE NONLINEARITIES FROM CASCADED THREE-WAVE MIXING

Cascaded nonlinearities in three-wave mixing crystals were noted long ago.[21] There a basic theoretical treatment predicted that under strongly phase-mismatched parametric interaction, the pump pulse may experience self-action, i.e., self-phase modulation of the spectrum. This is because for the simplest case of SHG, the strong phase mismatch $|\Delta k| \gg 0$ implies that the pump at $\omega_1$ will be partially upconverted to the second harmonic (SH) at $\omega_2 = 2\omega_1$ within a coherence length $l_{\mathrm{coh}} = \pi/|\Delta k|$, but after another coherence length the SH photons will be back converted to the pump. Under the strong phase-mismatch limit ($|\Delta k|L \gg 2\pi$), $l_{\mathrm{coh}}$ is much shorter than the crystal length $L$, so this up- and down-conversion process happens multiple times: this is the reason it is called a cascaded nonlinearity. The cascaded nonlinearity was first experimentally verified in Ref. 22, where the cascaded nonlinearity was shown to be tunable in sign and strength

$n_{2,\mathrm{casc}} \propto -d_{\mathrm{eff}}^2/\Delta k$, and where importantly it became clear that a self-defocusing effect was accessible ($n_{2,\mathrm{casc}} < 0$, requiring $\Delta k > 0$).

A controllable leading-order self-defocusing nonlinearity is quite unique, and quite some effort was therefore invested in applications of this effect in bulk crystals. One application was pulse compression of energetic pulses, because in bulk glasses the required spectral broadening was accompanied by self-focusing, limiting the pulse energy. The idea was to compensate for the material Kerr self-focusing, making $n_{2,\mathrm{eff}} < 0$ by using cascaded effects, and this would give a pulse compressor without filamentation limitations; it was first investigated in Ref. 23, where an SPM-induced self-defocusing spectral broadening was induced in a quadratic nonlinear crystal (BBO, beta-barium borate). The effective self-defocusing nonlinearity gave a negative chirp across the pulse, so the pulse could be compressed by passing it through a piece of bulk glass with positive normal dispersion.

A similar experiment was conducted by Ashihara *et al.*,[24] but instead of compressing the pulse "externally," they achieved soliton self-compression inside the crystal. This is because at the pump wavelength (800 nm from a TiSa amplifier) BBO has normal group-velocity dispersion (GVD), and for this sign of GVD, exciting a soliton requires $n_{2,\mathrm{eff}} < 0$. Although the soliton excitation was confirmed, the compression ratio was moderate. This is because BBO has a large group-velocity mismatch (GVM) between pump and SH at this wavelength, and indeed later experiments at longer wavelengths have shown few-cycle soliton self-compression in BBO due to a reduced GVM.[25,26]

Once the soliton has formed, it may become phase-matched to generate resonant radiation (i.e., a dispersive wave).[27] Since the self-defocusing soliton needs normal dispersion to form, the dispersive wave will naturally be generated in the anomalous dispersion regime, i.e., to the long-wavelength side.[28,29] This was recently experimentally verified in bulk BBO and LN,[20,26] and together with the soliton the dispersive wave(s) constitute the octave-spanning supercontinuum in the self-defocusing soliton case, which for LN can extend from 1.0 to 4.0 $\mu$m. This showed that the self-defocusing Kerr-like nonlinearity can be used as an efficient route towards high-energy filament free supercontinuum generation.

As mentioned above, LN, LIS, and similar crystals are advantageous because they use "non-critical" interaction, i.e., the so-called type 0 three-wave mixing, where pump and SH have the same polarization and the phase-matching conditions do not depend very much on angle (hence the name non-critical). The advantages are that one may exploit the large diagonal tensor components, e.g., the $d_{33}$ of LN, and that spatial walk-off is nil. For supercontinuum generation the added bonus is that the SH has the same polarization as the pump, so there can be a considerable harmonic extension of the continuum (multiple octaves have been observed in LN waveguides[30,31]). The disadvantages are that the intra-harmonic dispersion (i.e., between pump and SH) is very large (so $\Delta k$ and GVM are very big), and that phase-matching is impossible (impossible to get $\Delta k = 0$ and locate the SHG phase matching point as well as the maximum cascading point $\Delta k L = \pi$). Despite the large $\Delta k$, the cascading nonlinear index $n_{2,\mathrm{casc}} = -d_{\mathrm{eff}}^2/\Delta k$ can be quite significant: this is because $d_{\mathrm{eff}}$ is often very large and is thereby able to compensate for the large $\Delta k$. Importantly, for type 0 interaction $\Delta k > 0$ if pumped not too close to a UV absorption region, because the SH will always have a larger refractive index than the pump (remember $\Delta k \propto [n(\omega_2) - n(\omega_1)]$). This means that in type 0 the cascaded SHG nonlinearity in a bulk crystal will always be self-defocusing. The question is merely: is it strong enough to overcome the material Kerr nonlinearity and generate an effective self-defocusing effect? We can pose this limit as a figure-of-merit parameter FOM $= |n_{2,\mathrm{casc}}|/n_{2,\mathrm{Kerr}}$ and if FOM $> 1$ then the self-defocusing nonlinearity is dominating. LN has an FOM $> 1$ in the near-IR, as we used this to excite a temporal few-cycle soliton[19] when pumping in the normal GVD regime below its ZDW of 1.92 $\mu$m, followed by octave-spanning supercontinuum generation.[20]

Other work has appeared over the past years where broadband energetic pulses were generated in mid-IR quadratic nonlinear crystals. Recently, Ashihara and Kawahara[6] pumped GaAs in the mid-IR just below its ZDW to give significant spectral broadening (well over 2000 nm of bandwidth) at 5.0 $\mu$m. GaAs has a very large quadratic nonlinearity, and is as such a good cascading candidate for self-defocusing cascading, but we calculate its figure of merit to be less than unity, i.e., self-focusing is dominating, and this was also noted by the authors. Therefore the spectral broadening came purely from self-focusing SPM due to the high material $n_{2,\mathrm{Kerr}}$ of GaAs. In quadratic

nonlinear crystals it was also recently shown that adiabatic near-IR to mid-IR frequency conversion gives octave-spanning bandwidths with $\mu$J pulse energies.[32]

## III. LITHIUM THIOINDATE

Here we focus on the approach using the self-defocusing cascaded nonlinearity. Using LN as an inspiration, we recently calculated the figure of merit for a range of mid-IR crystals,[33] who all have very large diagonal tensor components and possibility of getting crystal cut for non-critical SHG. One of the main crystals that attracted our interest was LIS, because it has a ZDW around 3.53 $\mu$m, see Fig. 1, and an FOM $\simeq$ 2. Furthermore it is commercially available in quite big samples. Our simulations showed soliton formation and resonant radiation in the mid-IR, eventually giving supercontinuum radiation over several octaves in the mid-IR.

For the present experiment we used a commercially available LIS crystal (Moltech), 15 mm long and $6 \times 6$ mm$^2$ aperture. LIS belongs to the biaxial $mm2$ point group and our sample was cut with $\theta = 90°$ and $\phi = 0$. This gives a maximum quadratic nonlinearity $d_{\text{eff}} = d_{33}$ where $d_{33} = 16$ pm/V@2.3 $\mu$m.[34] This cut makes the SHG noncritical so both pump and SH have the same polarization (both are "slow" waves, with linear refractive index given by $n_Z$, see more details in Ref. 33). The SHG process is highly phase-mismatched (see Fig. 1, coherence length $l_{\text{coh}} = \pi/\Delta k \simeq 60$ $\mu$m), but notably not as much as in LN (where the coherence length can be an order of magnitude shorter). Due to the high quadratic nonlinearity the cascading Kerr nonlinear index is large ($n_{2,\text{casc}} = -2\omega_1 d_{\text{eff}}^2/[\varepsilon_0 c^2 n^2(\omega_1) n(\omega_2)\Delta k] \simeq -60 \cdot 10^{-20}$ m$^2/W$ in the pump range of interest). This competes with the material Kerr nonlinearity, and for LIS the cubic nonlinear

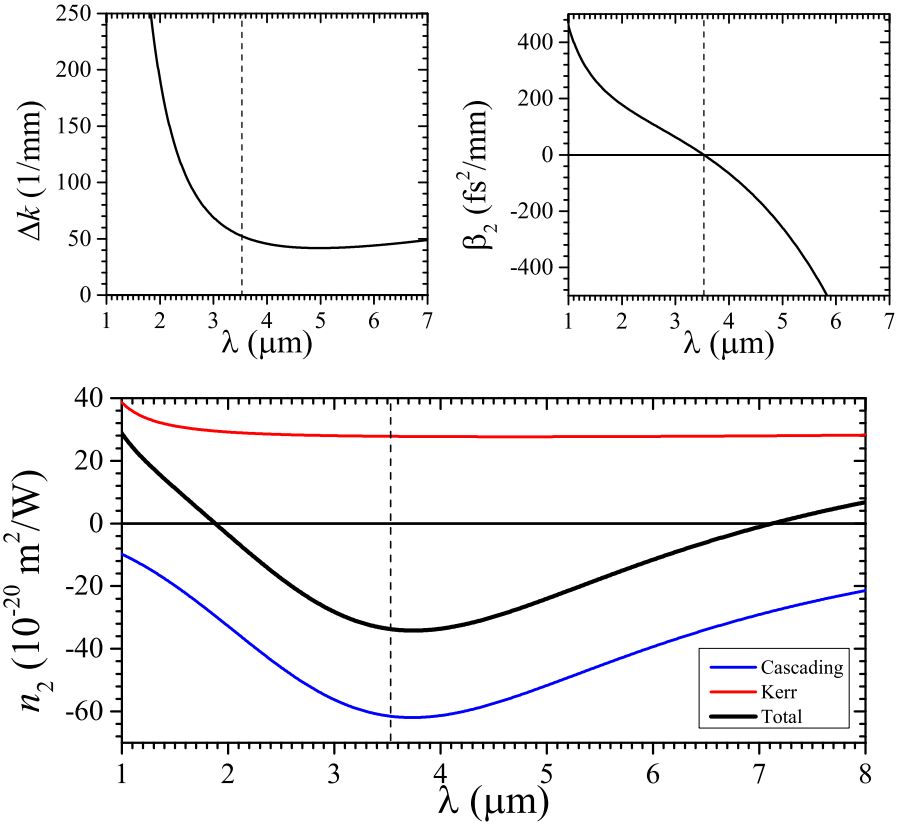


FIG. 1. Top: Phase-mismatch and GVD parameter. Bottom: Calculated cubic nonlinear refractive indices in LIS cut for interaction in the $XY$ plane ($\theta = \pi/2$ and $\phi = 0$); thus the cascading channel is $ss \rightarrow s$, where the pump polarization is along the slow index $n_Z$, and the Kerr SPM nonlinearity is calculated for the $sss \rightarrow s$ interaction. The vertical dashed line denotes the ZDW.

tensor components are not known. However, from its rather high bandgap along the $Z$ direction ($E_g = 3.55$ eV[34]) the two-band model (see Ref. 33 for details) estimates the Kerr nonlinearity to be around $+30 \cdot 10^{-20}$ m$^2$/W. We therefore expect the overall cubic nonlinearity to be self-defocusing. This is summarized in Fig. 1, which shows the wavelength dependence of the material and cascaded Kerr nonlinear indices, calculated as discussed in Ref. 33. In the range 2-7 $\mu$m the effective nonlinearity is predicted to be self-defocusing, and the deducted figure of merit (i.e., the ratio between the cascaded and Kerr nonlinearity) is as high as 2, very similar to LN.

The crystal was for various practical reasons uncoated, and therefore some end facet reflection loss occurred. These can easily be eliminated by a suitable broadband anti-reflection coating. We found that the crystal was remarkably resilient to the high intensities we used (up to 800 GW/cm$^2$), which we in part attribute to the short sub-100 fs pump pulse duration. No crystal damage was observed on short term time scales (we used the crystal 10 minutes at a time for the highest intensities) or on longer time scales (multiple hours) where more moderate intensities were used. Whether a coated crystal would have the same damage thresholds will have to be investigated.

## IV. RESULTS

We pumped the LIS crystal with 85 fs pulses in the 3.0-3.9 $\mu$m range from a commercial 1 kHz TiSa-amplifier based optical parametric amplifier (OPA) followed by a non-collinear difference-frequency generation stage. The maximum pulse energy was 50 $\mu$J inside the crystal, after taking into account Fresnel reflection losses. The pulses had around 200-250 nm bandwidth and were close to transform limit. The input beam was loosely focused (0.27 mm FWHM). Due to the lack of broadband mid-IR neutral density filters for fine, moderate attenuation, we controlled the mid-IR intensity by adjusting the pump power of the OPA. We note that for very low OPA (or mid-IR) output, there was some fluctuation regarding the output power, which is acceptable in this study since we only looked into the trends for the low intensities. The output was measured with an FPAS-1600 spectrometer (Infrared Systems) with a cooled MCT detector, and long-pass filters were used to selectively cover the 1-7 $\mu$m range.

The results for different pump intensities and pump wavelengths are summarized in Fig. 2. Generally, we needed around 150 GW/cm$^2$ to see an octave-spanning supercontinuum, i.e., around

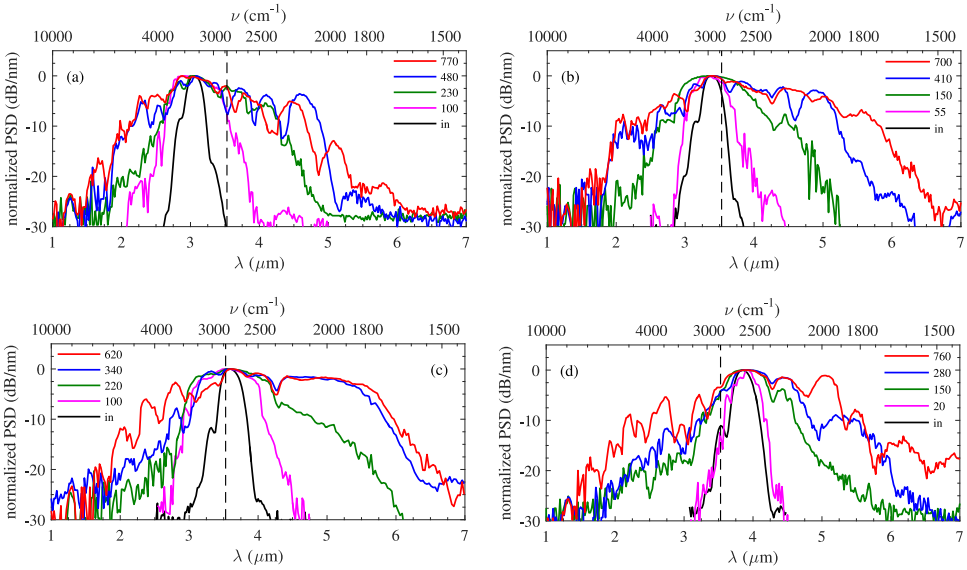


FIG. 2. Experimentally recorded supercontinua in 15 mm LIS for pump wavelengths of (a) $\lambda = 3.05$ $\mu$m, (b) 3.39 $\mu$m, (c) 3.60 $\mu$m, and (d) 3.86 $\mu$m, and for various pump intensities (indicated in GW/cm$^2$). The power spectral density (PSD) normalized to its peak value is shown. The vertical dashed line denotes the ZDW. The top axis shows the frequency in inverse wavenumbers $\nu = 1/\lambda$, as often used in spectroscopy. Note the absorption dip at the $CO_2$ line ($\nu \simeq 2,400$ cm$^{-1}$).

10 $\mu$J of pulse energy. The bandwidths in the maximum peak power cases exceed 2 octaves (1.6-7.0 $\mu$m@ − 20 dB for $\lambda = 3.86$ $\mu$m pump). For the two cases that used pumping close to the ZDW, the supercontinuum is very flat across the central range, while in the two cases pumping further away the supercontinuum is more modulated.

The broadest supercontinuum was observed when pumping above the ZDW. This is surprising as we would have expected the broadest supercontinuum in the soliton case, i.e., when pumping below the ZDW. The soliton itself is namely very broadband (typically close to single cycle duration is observed in simulations at the soliton self-compression stage) and is furthermore also able to excite the resonant radiation in the anomalous dispersion regime above the ZDW, which further extends the bandwidth. We believe the explanation lies in the proximity of the pump wavelength to the ZDW, which means that even when pumping above the ZDW the early stage spectral broadening leaks into the normal dispersion regime. When the most intense pulses were applied this allows a soliton to form despite pumping in the non-solitonic regime (and as such it is kind of the reverse case recently found in Refs. 26 and 28).

Numerical simulations were used to understand the experimental data. These were based on the so-called nonlinear analytic envelope equation,[35,36] which is an envelope-like approach that is actually modeling the carrier wave, and has therefore sub-carrier wave resolution, and it includes a complete expansion of the nonlinear terms. The model was recently extended to include both quadratic, cubic and delayed Raman effects, and its details can be found in Ref. 37; the model we use is based on Eq. (31) there. The Raman mode was taken the same as in Ref. 33, and the best agreements with the experimental results were seen using $n_{2,\mathrm{Kerr}} = 50 \cdot 10^{-20}$ m$^2$/W and a Raman fraction $f_R = 0.2$; this implies that the electronic Kerr nonlinearity is $40 \cdot 10^{-20}$ m$^2$/W, quite close to the value predicted by the two-band model in Fig. 1. The simulations neglected diffraction and this plane-wave approximation is typically justified in the effective self-defocusing regime of bulk quadratic nonlinear crystals even for moderate-to-high intensities. Generally, this means that while a detailed spatio-temporal dynamics investigation is not done, the overall main dynamics is dominated by the on-axis contribution that is well modeled by the plane-wave approximation. This avoids a cumbersome full 3+1D simulation that can be very time consuming considering that the model has to have attosecond-scale time resolution. Finally, we note that for the selected cut LIS has no SHG coupling to the orthogonal polarization (for the $ss \rightarrow f$ channel $d_{\mathrm{eff}} = 0$). As the cubic tensor components are taken isotropic, they do not have any cross-polarization coupling either, so we only need to model the input $s$ polarization.

A specific simulation example is shown in Fig. 3, where we chose $\lambda = 3.05$ $\mu$m and a moderate intensity, corresponding to the green curve in Fig. 2(a). The time domain in (a) and (b) shows that a self-compressed soliton forms after 11 mm, but it is accompanied with two minor satellite pulses. Such pulse splitting may be caused by competing nonlinearities to the SPM from a combination of the Raman effect and self-steepening.[19,38,39] Especially the self-steepening can become strong in cascading since it contributes to the intrinsic Kerr-induced self-steepening with a scaling factor $d_{12}/\Delta k$, i.e., the ratio between GVM and phase mismatch.[38,40,41] In the spectral domain, significant spectral broadening occurs up to the self-compression point, and after this stage a broadband dispersive wave forms in the range 4.0-5.0 $\mu$m. This peak can also be noticed in the experimental spectrum in Fig. 2(a). Towards shorter wavelengths the second- and third-harmonic spectra are evident, although the latter is quite weak. Notice that the harmonic spectra (located around the second- and third-harmonic frequencies) also show continuum generation; this is because they are not phase-matched, and in the cascading limit the harmonic spectrum is "slaved" or "locked" to the pump spectrum.[40,42,43] In some sense, since these harmonics have the same polarization as the pump, this is a harmonic extension of the mid-IR supercontinuum formed at the pump wavelength, but as the phase-mismatch coefficients are large the energy is quite low. It is important to emphasize here that the nonlinearity behind the mid-IR supercontinuum is an effective Kerr-like nonlinearity, mediated by the phase-mismatched SHG effect. Exactly because everything is so far from phase matching, the new colors generated in the supercontinuum will not easily find phase-matching through, e.g., three-wave mixing, to new frequencies. They would otherwise show up as sharp resonant lines in the low-wavelength part of the spectrum, which we did not observe.

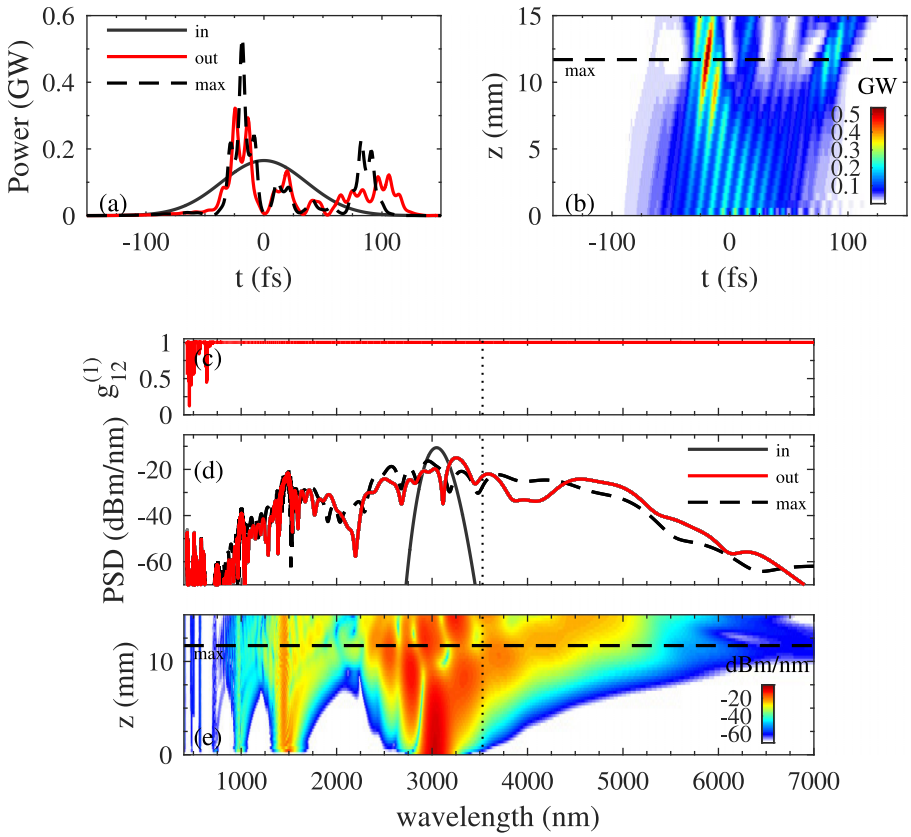


FIG. 3. Numerical simulation at $\lambda = 3.05\ \mu$m with 200 GW/cm$^2$ peak input intensity. (a) and (b) show the temporal evolution and (d) and (e) the spectral evolution of a single noise realization. In each case the "max" case shows the cut for maximum peak power in time domain, i.e., where the soliton self-compresses after 11 mm propagation. The output PSD in (d) and the coherence function $g^{(1)}_{12}$ in (e) were averaged over 20 noise realizations. The modulations on the envelope in (a) and (b) are caused by harmonic generation along the polarization direction of the pump since this is included in the numerical model.

Figure 4 compares simulations for the $\lambda_1 = 3.39\ \mu$m case qualitatively with the experimental data for different intensities. The simulations show a good agreement concerning the spectral bandwidth, especially in the mid-IR. In the near-IR the simulations have a clear peak at the SH wavelength (although it becomes somewhat blue-shifted at high intensities, an effect that is already apparent in Fig. 3(e) despite the moderate intensity used there), and the experimental data do not show this. This could be because the simulations overestimate the SH power. The plane-wave simulation namely only models the on-axis distribution, while in the experiment the aperture of the mid-IR monochromator was quite big so it essentially records a spatial average over most of the beam. This makes it more difficult to compare the two cases than in a standard near-IR setup where fiber tips can be used to collect the on-axis intensity distribution.

In the numerical simulations noise was used to gauge the coherence of the spectra.[44] Our noise source is slightly different than the usual one-photon-per-mode approach used in Ref. 44, so let us elaborate a bit on the details. The noise source we used corresponds to the quantum fluctuations in the vacuum state according to the Wigner representation.[45–47] The advantage of the Wigner representation (compared to P or Q) is that the noise is additive and is only added in the initial condition; this means that the standard split-step routine based on Runge-Kutta solvers can be used. Conversely more rigorous Langevin solvers like the Heun method are needed for the multiplicative noise of the P and Q representation, i.e., where noise must be added at every $z$ step. In order to model the vacuum state in the Wigner representation, a half photon per temporal mode is added to the initial condition with Gaussian white noise distribution.[47] This approach is different than the usual one-photon-per-mode approach,[44] which adds a Gaussian distributed phase noise in the

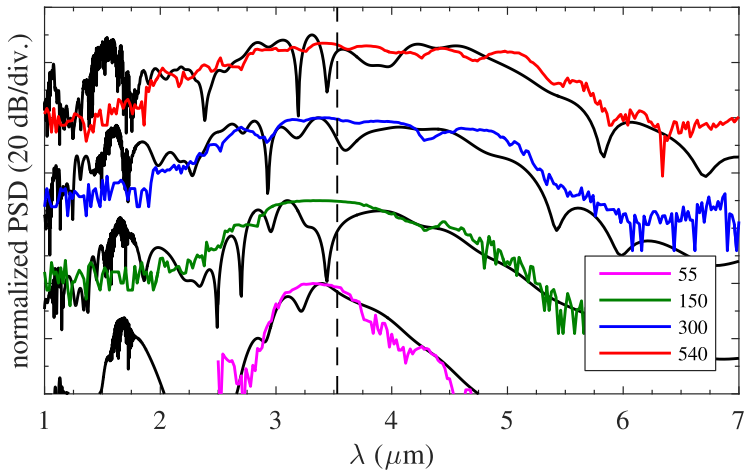


FIG. 4. Normalized PSD at the crystal exit, comparing numerical simulations and experimental results for $\lambda_1 = 3.39\ \mu$m. A 30 dB offset per dataset was used to make the plot easier to read. The experimental intensities in GW/cm$^2$ are shown in the legend, and the numerical simulations (black lines) used similar intensities.

frequency domain with 1 photon per frequency mode average energy density. In time domain this approach has on average $2\pi$ half photons per mode; this does not conform with the vacuum fluctuations of the Wigner model. That being said, technically the two approaches are almost identical as both add noise as an initial condition. In our case we add on average half a photon per temporal mode, while in Ref. 44 on average one photon is added per frequency mode to the spectral phase.

With this noise implementation, the coherence analysis was conducted as in Ref. 44: we repeated each simulation case a suitable number of times with different initial noise realizations. Each noise realization represents a single pump shot in the experiment. The first order spectral coherence function $g_{12}^{(1)}(\lambda)$ was then calculated, and we found the coherence of the spectra to be excellent: an example is shown in Fig. 3(c) where the spectral coherence function is unity across the generated supercontinuum. When the coherence is unity at a given wavelength the supercontinuum energy does not fluctuate from shot to shot. We even attempted to add an additional significantly stronger noise source than the vacuum fluctuations (i.e., noise from the amplification stage or technical noise sources, all modeled in the same way as a Gaussian white noise but with many photons per temporal mode), and the high coherence still pertained.

We also attempted, along the lines of the results shown in Refs. 19 and 24–26, to measure a self-compressed soliton with a home-built intensity autocorrelator. However, we were not able to find clear signs of a clean compressed soliton, and to understand this, the detailed numerical simulations in Fig. 3 show multiple pulse splitting. This means that a single compressed pulse is rarely seen and instead two or more short pulses form, which are much harder to detect with an autocorrelation unit. We hope in the future to do more detailed frequency-resolved time-correlation traces to investigate the precise chirp across the pulse.

In the experiment we also characterized the transverse cross section of the supercontinuum with an uncooled microbolometer camera. The camera is sensitive in the entire range of the recorded supercontinua. The measurements were done around 20 cm from the exit of the crystal, and from the beam waist size of the input beam ($w_0 = 0.2$ mm) we estimate that the distance $z/z_R \simeq 5$, i.e., 5 times the Rayleigh length. This places the camera in the Fresnel diffraction zone. The evolution of the beam vs. intensity showed formation of a more narrow spot in the center. Although this was not a near-field measurement, it does indicate diffraction for high intensities. This could be related to the pulse compression but it might also indicate that the self-defocusing cascading and self-focusing material Kerr effects are competing and give nontrivial spatio-temporal coupling.

That being said, the spectra and the spatial characterization did not reveal any fluctuations in the transverse beam profile on a shot-to-shot level and the long-term stability was good. Thus, despite the diffraction that we observed, the generated supercontinua are stable and should be

quite useful for spectroscopy. We indeed verified that the supercontinuum could be used to do simple absorption measurements: by passing the supercontinuum through an LN crystal, we could reconstruct transmission curves quite similar to FTIR measurements of the crystal (in particular the 4-6 $\mu$m mid-IR absorption edge matched very well). Moreover, while using the LIS crystal in an actual mid-IR pump-probe spectroscopy setup (results to be published elsewhere) we were able to measure the beam profile far away from the crystal, essentially in the far field (Fraunhofer zone), and a clean Gaussian-like profile was observed with only minor weak rings away from the core peak.

The energies in the broadest supercontinua were measured to be up to 30 $\mu$J, i.e., retaining over half the pump energy. For somewhat lower intensities this ratio increased further. Basically, the energy transfer from the pump into the supercontinuum is highly efficient, and the main "loss" channels are coming from Fresnel reflections at the end facet, stemming from the crystal end facet being uncoated, energy transferred to the SH and higher harmonics, as well as diffraction effects. We believe reduced diffraction for lower intensities is the main reason why we there were able to retain more energy in the supercontinuum. Scaling up the energy should be straightforward as the effective nonlinearity is self-defocusing; basically one would simply keep the same pump intensity and defocus the beam spot. Such an energy upscaling also promises a mid-IR supercontinuum with an energy on the mJ level.

## V. CONCLUSION

We have experimentally demonstrated multiple-octave spanning supercontinuum generation by pumping a bulk lithium thioindate (LIS) crystal in the 3.0-3.9 $\mu$m range with bright 50 $\mu$J 85 fs pulses. The crystal was pumped with a loosely focused 0.27 mm diameter beam and the onset of a supercontinuum (octave spanning) was typically around 150 GW/cm$^2$, i.e., around 10 $\mu$J of pulse energy. The crystal was cut for noncritical phase-mismatched SHG, giving a strong self-defocusing nonlinearity. We did see indications of diffraction in the transverse part of the beam at high intensities. This was recorded at an intermediate distance from the crystal (Fresnel zone), while another measurement further away from the crystal (Fraunhofer zone) did not show significant diffraction effects. We will in future experiments look further into this. This notwithstanding, the supercontinua at high intensities did not reveal any significant spatial fluctuations and should therefore be quite useful for ultrafast spectroscopy. Moreover, we emphasize that the energy in the supercontinuum can easily be scaled up by simply using a larger pump beam diameter, and already in the present state with around 30 $\mu$J energy it should be energetic enough to be used as an ultra-broadband mid-IR pump in a femtosecond pump-probe experiment. The broadest spectrum spanned the range from 1.6 to 7.0 $\mu$m, enough to cover the entire range of fundamental vibrational frequencies of hydrogen and carbon-type bonds, including the near-IR part needed to cover their first overtones. We note that the overtones can be reached by the supercontinuum, thus opening for new possibilities in ultrafast mid-IR vibrational spectroscopy. The technique we used to generate the supercontinuum can readily be used in other mid-IR quadratic nonlinear crystals as well, which means that different parts of the mid-IR can be covered, especially the fingerprint region from 6 to 12 $\mu$m, by pumping similar crystals at longer wavelengths.

## ACKNOWLEDGMENTS

This work has been supported by the Danish Council for Independent Research (Grant Nos. 11-106702 and 4070-00114B). We thank Poul B. Petersen, Ashley Stingel, Heather Vanselous, Satoshi Ashihara, Valentin Petrov, Jens Biegert, and Cord Arnold for fruitful discussions.

[1] *The Supercontinuum Laser Source*, 2nd ed., edited by R. R. Alfano (Springer, New York, 2006).
[2] C. Calabrese, A. M. Stingel, L. Shen, and P. B. Petersen, "Ultrafast continuum mid-infrared spectroscopy: Probing the entire vibrational spectrum in a single laser shot with femtosecond time resolution," Opt. Lett. **37**, 2265–2267 (2012).
[3] J. M. Dudley, G. Genty, and S. Coen, "Supercontinuum generation in photonic crystal fiber," Rev. Mod. Phys. **78**, 1135 (2006).

[4] B. Prade, M. Franco, A. Mysyrowicz, A. Couairon, H. Buersing, B. Eberle, M. Krenz, D. Seiffer, and O. Vasseur, "Spatial mode cleaning by femtosecond filamentation in air," Opt. Lett. **31**, 2601–2603 (2006).
[5] P. B. Corkum, P. P. Ho, R. R. Alfano, and J. T. Manassah, "Generation of infrared supercontinuum covering 3–14 $\mu$m in dielectrics and semiconductors," Opt. Lett. **10**, 624–626 (1985).
[6] S. Ashihara and Y. Kawahara, "Spectral broadening of mid-infrared femtosecond pulses in GaAs," Opt. Lett. **34**, 3839–3841 (2009).
[7] F. Silva, D. Austin, A. Thai, M. Baudisch, M. Hemmer, D. Faccio, A. Couairon, and J. Biegert, "Multi-octave supercontinuum generation from mid-infrared filamentation in a bulk crystal," Nat. Commun. **3**, 807 (2012).
[8] D. Kartashov, S. Ališauskas, A. Pugžlys, A. Voronin, A. Zheltikov, M. Petrarca, P. Béjot, J. Kasparian, J.-P. Wolf, and A. Baltuška, "White light generation over three octaves by femtosecond filament at 3.9 $\mu$m in argon," Opt. Lett. **37**, 3456–3458 (2012).
[9] J. Darginavičius, D. Majus, V. Jukna, N. Garejev, G. Valiulis, A. Couairon, and A. Dubietis, "Ultrabroadband supercontinuum and third-harmonic generation in bulk solids with two optical-cycle carrier-envelope phase-stable pulses at 2 $\mu$m," Opt. Express **21**, 25210–25220 (2013).
[10] H. Liang, P. Krogen, R. Grynko, O. Novak, C.-L. Chang, G. J. Stein, D. Weerawarne, B. Shim, F. X. Kärtner, and K.-H. Hong, "Three-octave-spanning supercontinuum generation and sub-two-cycle self-compression of mid-infrared filaments in dielectrics," Opt. Lett. **40**, 1069–1072 (2015).
[11] O. Mouawad, P. Béjot, F. Billard, P. Mathey, B. Kibler, F. Désévédavy, G. Gadret, J.-C. Jules, O. Faucher, and F. Smektala, "Mid-infrared filamentation-induced supercontinuum in As-S and an As-free Ge-S counterpart chalcogenide glasses," Appl. Phys. B **121**, 433–438 (2015).
[12] A. A. Lanin, A. A. Voronin, E. A. Stepanov, A. B. Fedotov, and A. M. Zheltikov, "Multioctave, 3–18 $\mu$m sub-two-cycle supercontinua from self-compressing, self-focusing soliton transients in a solid," Opt. Lett. **40**, 974–977 (2015).
[13] T. Fuji and T. Suzuki, "Generation of sub-two-cycle mid-infrared pulses by four-wave mixing through filamentation in air," Opt. Lett. **32**, 3330–3332 (2007).
[14] P. B. Petersen and A. Tokmakoff, "Source for ultrafast continuum infrared and terahertz radiation," Opt. Lett. **35**, 1962–1964 (2010).
[15] T. Fuji, J. Rauschenberger, A. Apolonski, V. S. Yakovlev, G. Tempea, T. Udem, C. Gohle, T. W. Hänsch, W. Lehnert, M. Scherer, and F. Krausz, "Monolithic carrier-envelope phase-stabilization scheme," Opt. Lett. **30**, 332–334 (2005).
[16] N. M. N. Srinivas, S. S. Harsha, and D. N. Rao, "Femtosecond supercontinuum generation in a quadratic nonlinear medium (KDP)," Opt. Express **13**, 3224–3229 (2005).
[17] R. S. S. Kumar, S. S. Harsha, and D. N. Rao, "Broadband supercontinuum generation in a single potassium di-hydrogen phosphate (KDP) crystal achieved in tandem with sum frequency generation," Appl. Phys. B **86**, 615–621 (2007).
[18] K. Krupa, A. Labruyère, A. Tonello, B. M. Shalaby, V. Couderc, F. Baronio, and A. B. Aceves, "Polychromatic filament in quadratic media: Spatial and spectral shaping of light in crystals," Optica **2**, 1058–1064 (2015).
[19] B. B. Zhou, A. Chong, F. W. Wise, and M. Bache, "Ultrafast and octave-spanning optical nonlinearities from strongly phase-mismatched quadratic interactions," Phys. Rev. Lett. **109**, 043902 (2012).
[20] B. Zhou, H. Guo, and M. Bache, "Energetic mid-IR femtosecond pulse generation by self-defocusing soliton-induced dispersive waves in a bulk quadratic nonlinear crystal," Opt. Express **23**, 6924–6936 (2015).
[21] L. A. Ostrovskii, "Self-action of light in crystals," Pis'ma Zh. Eksp. Teor. Fiz. **5**, 331 (1967); JETP Lett. **5**, 272–275 (1967).
[22] R. DeSalvo, D. Hagan, M. Sheik-Bahae, G. Stegeman, E. W. Van Stryland, and H. Vanherzeele, "Self-focusing and self-defocusing by cascaded second-order effects in KTP," Opt. Lett. **17**, 28–30 (1992).
[23] X. Liu, L.-J. Qian, and F. W. Wise, "High-energy pulse compression by use of negative phase shifts produced by the cascaded $\chi^{(2)}:\chi^{(2)}$ nonlinearity," Opt. Lett. **24**, 1777–1779 (1999).
[24] S. Ashihara, J. Nishina, T. Shimura, and K. Kuroda, "Soliton compression of femtosecond pulses in quadratic media," J. Opt. Soc. Am. B **19**, 2505–2510 (2002).
[25] J. Moses and F. W. Wise, "Soliton compression in quadratic media: High-energy few-cycle pulses with a frequency-doubling crystal," Opt. Lett. **31**, 1881–1883 (2006).
[26] B. Zhou and M. Bache, "Dispersive waves induced by self-defocusing temporal solitons in a beta-barium-borate crystal," Opt. Lett. **40**, 4257–4260 (2015).
[27] D. V. Skryabin and A. V. Gorbach, "Colloquium: Looking at a soliton through the prism of optical supercontinuum," Rev. Mod. Phys. **82**, 1287–1299 (2010).
[28] M. Bache, O. Bang, B. B. Zhou, J. Moses, and F. W. Wise, "Optical Cherenkov radiation in ultrafast cascaded second-harmonic generation," Phys. Rev. A **82**, 063806 (2010).
[29] M. Bache, O. Bang, B. B. Zhou, J. Moses, and F. W. Wise, "Optical Cherenkov radiation by cascaded nonlinear interaction: An efficient source of few-cycle energetic near-to mid-IR pulses," Opt. Express **19**, 22557–22562 (2011).
[30] C. Langrock, M. M. Fejer, I. Hartl, and M. E. Fermann, "Generation of octave-spanning spectra inside reverse-proton-exchanged periodically poled lithium niobate waveguides," Opt. Lett. **32**, 2478–2480 (2007).
[31] C. R. Phillips, C. Langrock, J. S. Pelc, M. M. Fejer, J. Jiang, M. E. Fermann, and I. Hartl, "Supercontinuum generation in quasi-phase-matched $LiNbO_3$ waveguide pumped by a Tm-doped fiber laser system," Opt. Lett. **36**, 3912–3914 (2011).
[32] H. Suchowski, P. R. Krogen, S.-W. Huang, F. X. Kärtner, and J. Moses, "Octave-spanning coherent mid-IR generation via adiabatic difference frequency conversion," Opt. Express **21**, 28892–28901 (2013).
[33] M. Bache, H. Guo, and B. Zhou, "Generating mid-IR octave-spanning supercontinua and few-cycle pulses with solitons in phase-mismatched quadratic nonlinear crystals," Opt. Mater. Express **3**, 1647–1657 (2013).
[34] S. Fossier, S. Salaün, J. Mangin, O. Bidault, I. Thénot, J.-J. Zondy, W. Chen, F. Rotermund, V. Petrov, P. Petrov, J. Henningsen, A. Yelisseyev, L. Isaenko, S. Lobanov, O. Balachninaite, G. Slekys, and V. Sirutkaitis, "Optical, vibrational, thermal, electrical, damage, and phase-matching properties of lithium thioindate," J. Opt. Soc. Am. B **21**, 1981–2007 (2004).
[35] M. Conforti, F. Baronio, and C. De Angelis, "Nonlinear envelope equation for broadband optical pulses in quadratic media," Phys. Rev. A **81**, 053841 (2010).

[36] M. Conforti, A. Marini, T. X. Tran, D. Faccio, and F. Biancalana, "Interaction between optical fields and their conjugates in nonlinear media," Opt. Express **21**, 31239–31252 (2013).
[37] M. Bache, "The nonlinear analytical envelope equation in quadratic nonlinear crystals" (2016), e-print arXiv:1603.00188.
[38] J. Moses and F. W. Wise, "Controllable self-steepening of ultrashort pulses in quadratic nonlinear media," Phys. Rev. Lett. **97**, 073903 (2006).
[39] H. Guo, X. Zeng, B. Zhou, and M. Bache, "Nonlinear wave equation in frequency domain: Accurate modeling of ultrafast interaction in anisotropic nonlinear media," J. Opt. Soc. Am. B **30**, 494–504 (2013).
[40] M. Bache, O. Bang, J. Moses, and F. W. Wise, "Nonlocal explanation of stationary and nonstationary regimes in cascaded soliton pulse compression," Opt. Lett. **32**, 2490–2492 (2007).
[41] F. Ö. Ilday, K. Beckwitt, Y.-F. Chen, H. Lim, and F. W. Wise, "Controllable Raman-like nonlinearities from nonstationary, cascaded quadratic processes," J. Opt. Soc. Am. B **21**, 376–383 (2004).
[42] G. Valiulis, V. Jukna, O. Jedrkiewicz, M. Clerici, E. Rubino, and P. DiTrapani, "Propagation dynamics and X-pulse formation in phase-mismatched second-harmonic generation," Phys. Rev. A **83**, 043834 (2011).
[43] B. Zhou, H. Guo, and M. Bache, "Soliton-induced nonlocal resonances observed through high-intensity tunable spectrally compressed second-harmonic peaks," Phys. Rev. A **90**, 013823 (2014).
[44] J. M. Dudley and S. Coen, "Coherence properties of supercontinuum spectra generated in photonic crystal and tapered optical fibers," Opt. Lett. **27**, 1180–1182 (2002).
[45] M. J. Werner, M. G. Raymer, M. Beck, and P. D. Drummond, "Ultrashort pulsed squeezing by optical parametric amplification," Phys. Rev. A **52**, 4202–4213 (1995).
[46] M. J. Werner and P. D. Drummond, "Pulsed quadrature-phase squeezing of solitary waves in $\chi^{(2)}$ parametric waveguides," Phys. Rev. A **56**, 1508–1518 (1997).
[47] E. Brambilla, A. Gatti, M. Bache, and L. A. Lugiato, "Simultaneous near-field and far field spatial quantum correlations in the high gain regime of parametric down-conversion," Phys. Rev. A **69**, 023802 (2004).